A Composition-Dependent Molecular Clutch Between T Cell Signaling Clusters and Actin

Jonathon A. Ditlev[1,2,*], Anthony R. Vega[3,*], Darius V. Köster[1,4,*], Xiaolei Su[1,5], Ashley M. Lakoduk[6], Ronald D. Vale[1,5], Satyajit Mayor[1,4,‡], Khuloud Jaqaman[3,7,‡], Michael K. Rosen[1,2,‡]

[1] The Howard Hughes Medical Institute Summer Institute, Marine Biological Laboratory, Woods Hole, MA, 02543, USA

[2] Department of Biophysics and Howard Hughes Medical Institute, University of Texas Southwestern Medical Center, Dallas, TX, 75390, USA

[3] Department of Biophysics, University of Texas Southwestern Medical Center, Dallas, TX, 75390, USA

[4] National Centre for Biological Sciences, Tata Institute for Fundamental Research, Bangalore, 560065, India

[5] Department of Cellular and Molecular Pharmacology and Howard Hughes Medical Institute, University of California, San Francisco, CA 94158, USA

[6] Department of Cell Biology, University of Texas Southwestern Medical Center, Dallas, TX, 75390, USA

[7] Lyda Hill Department of Bioinformatics, University of Texas Southwestern Medical Center, Dallas, TX, 75390, USA

[‡]Corresponding author. E-mail: mayor@ncbs.res.in (S.M.); khuloud.jaqaman@utsouthwestern.edu (K.J.); michael.rosen@utsouthwestern.edu (M.K.R.)

[*]These authors contributed equally to this work.

One-sentence summary: Compositional changes alter T cell signaling cluster binding to actin, enabling cluster propulsion by distinct actin networks.

Abstract

During T cell activation, phase-separated signaling protein clusters are moved toward the center of the immunological synapse by two distinct, concentric actin networks. How clusters move with actin is unknown. We observed that clusters lose the adaptor protein Nck as the clusters move across the boundary of the two actin networks. Biochemically reconstituted clusters with weak actin binders, Nck and its ligand N-WASP, promoted the strong association and movement of clusters with mobile actomyosin filaments. Clusters lacking these components were instead propelled by mechanical interactions. Basic elements of Nck and N-WASP coupled clusters to actin *in vitro*, and clusters constitutively containing basic elements moved aberrantly in cells. We propose that Nck and N-WASP act as a clutch between clusters and actin, and that changes in composition of these condensates enable cluster movement by the distinct dynamics of actin networks in different regions of the immunological synapse.

Introduction

Many cell surface receptors and their binding partners are organized into submicron- or micron-sized clusters on the cell membrane (*1*–*4*). Some of these clusters form through two-dimensional phase-separation driven by multivalent interactions between proteins containing multiple binding elements (*5*–*8*). This phenomenon is observed at the immunological synapse (IS), the interface of the T cell with an antigen presenting cell, which forms during T cell activation. There, the transmembrane adaptor protein LAT (linker for activation of T cells) and its intracellular binding partners Grb2, Sos1, SLP-76, Nck, and WASP, coalesce into phase-separated clusters at the membrane (*7*). The clusters that form in the distal supramolecular activating cluster (dSMAC) at the edge of the IS move radially through the peripheral SMAC (pSMAC) to the central SMAC (cSMAC) at the center of the IS. This movement is essential for proper T cell response to antigen presenting cells (*9*–*12*).

Translocation of LAT clusters from the dSMAC to the cSMAC is driven by motion of the actin cytoskeleton (*13*–*16*). Recent work has shown that two actin networks are generated at the IS in activated T cells (*17*, *18*). In the outer ~1/3 of the synapse, the Arp2/3 complex generates a dendritic actin meshwork, where the filaments are on average directed radially, perpendicular to the synapse edge. In the medial region closer to the cSMAC, this meshwork is largely replaced by formin-generated contractile actin arcs that are directed parallel to the synapse edge (Fig. S1) (*17*, *19*). Both filament networks move through the action of myosin motors as the cell-cell conjugate matures; however, the nature of this movement is different in the two cases. The dendritic network moves in a direction perpendicular to the edge of the synapse in a process termed retrograde flow (*13*–*16*), analogous to actin flow observed at the leading edge of migrating cells (*20*, *21*). In contrast, the contractile arcs sweep toward the center of the synapse in a telescoping manner and appear to have components of motion both perpendicular and parallel to the synapse edge (*18*).

It has remained unknown how LAT clusters engage actin to move across the synapse, and additionally, how clusters can move in a continuous radial direction through the action of two actin networks moving in different directions. To address these questions, we analyzed the interactions between LAT clusters and actin in cells and in reconstituted biochemical systems using quantitative microscopy and statistical analyses. These studies revealed that the phase separated LAT clusters recruit weak binders of actin filaments, Nck and N-WASP, thereby allowing the clusters to stably associate with actin filaments. By modulating the concentration of Nck, these clusters have different modes of engaging actin networks, and that switching between modes likely enables clusters to move radially through the action of two different actin networks at the IS.

LAT cluster composition changes as clusters traverse the IS

To investigate the composition of LAT clusters as they move across the plasma membrane in live, activated Jurkat T cells, we co-expressed LAT-mCitrine with Grb2-mCherry or LAT-mCherry with Nck-sfGFP. These cells bound to and spread on planar lipid bilayers coated with mobile ICAM-1 and an antibody to CD3, OKT3, producing an IS mimic with the bilayer. We used total internal reflection fluorescence (TIRF) microscopy to capture images of activated cells every 5 seconds for up to 5 minutes. We then automatically detected and tracked clusters containing LAT from their formation in the periphery of the IS to their coalescence with the cSMAC (using u-track; (*22*)), monitoring the fluorescence intensity of LAT and Grb2 or Nck in the clusters. Grb2 co-localized with LAT clusters at the edge of the synapse (Fig. 1A, movie S1) and its fluorescence intensity in the clusters was maintained throughout the trajectory to the center of the synapse (Fig. 1B, C). Nck also co-localized with LAT clusters at the edge of the synapse (Fig. 1D, movie S2). However, in contrast to Grb2, Nck fluorescence diminished relative to LAT during the trajectory. This intensity decrease began at 0.6-0.7 of the distance

from the center of the synapse to the synapse edge (referred to hereafter as "normalized radial position," equal to zero at the synapse center and 1 at the synapse edge; see Supplemental Methods) (Fig. 1C, E). The emergence of this pattern from averaging 207 tracks suggests that spatial position is a key determinant of Nck residence in LAT clusters. In contrast, when the clusters were aligned according to their appearance time (Fig. S2), Nck intensity steadily decreased over the course of the trajectory across the IS without any characteristic start time (beyond t = 0). This suggests that in this experimental setting, position plays a more instructive role than time in determining the residence of Nck in clusters. However, since time and space are coupled, our data do not rule out a role for time in this process, as has previously been observed in experimental conditions where LAT clusters were immobilized (*23*).

The normalized radial position at which LAT clusters started to lose Nck roughly coincided with the region where the actin network has been reported to switch from dendritic architecture to arc architecture (*17*–*19*). Nck binds directly to WASP-family proteins, which in turn have been reported to bind actin filament barbed ends through their WH2 domains (*24*, *25*). Since the loss of Nck occurred shortly before the reported change in actin network architecture, we hypothesized that the change in LAT cluster composition might allow the clusters to interact differently with the two actin networks that they encounter while traversing the IS.

Composition regulates the interaction of LAT clusters with actin networks

To test our hypothesis that the composition of phase-separated LAT clusters alters their ability to interact with actin filaments, we biochemically reconstituted clusters of various compositions on planar lipid bilayers coated with actin filaments (Fig. 2A). We attached polyhistidine-tagged phospho-LAT (pLAT) and polyhistidine-tagged actin-binding domain of ezrin (eABD) to Ni-NTA functionalized lipids within the bilayer. For experiments involving actin, we added polymerized actin filaments that bound to the bilayer via the eABD. To induce actin filament movement we

added muscle myosin II and ATP, as previously described (*26*). Finally, we induced LAT cluster formation by adding an increasing subset of binding partners, in the order Grb2, Sos1, phospho-SLP-76 (pSLP-76), Nck, and, finally, N-WASP, as previously described (*7*). Hereafter we use the nomenclature pLAT → X to indicate clusters containing pLAT and all binding partners up to X (e.g. if X is Nck, then the clusters would contain pLAT, Grb2, Sos1, pSLP-76 and Nck). We induced cluster formation without actin, with actin alone, or with active actomyosin networks (Fig 2B, movies S3, S4, and S5). We immediately observed that clusters containing Nck or Nck and N-WASP associated with and wet actin filaments in both actin networks alone and actomyosin networks, while clusters lacking these proteins remained distributed across the bilayer (Fig 2B). As a corollary, co-localization analysis showed that actin is more strongly enriched in clusters that contain Nck and N-WASP than in clusters lacking these proteins (Fig 2C).

In all conditions we automatically detected clusters and tracked their movement on the bilayer for 15 minutes and classified cluster movement using Moment Scaling Spectrum analysis of cluster displacements ((*22*, *27*, *28*); see Supplemental Methods). This analysis revealed that LAT clusters were either immobile, confined (i.e. moved within a confinement region), or mobile (i.e. moved without apparent restrictions, in a manner akin to free diffusion). When clusters were formed on bilayers without actin, 80% of clusters showed little movement; they were either immobile or confined, in an area of radius 100-150 nm (Fig 2D, E, movie S3). Cluster mobility was similar for all compositions. When LAT clusters were formed within actin networks in the absence of myosin, cluster movement varied with composition. pLAT → Sos1 and pLAT → pSLP76 clusters showed an increase in apparent diffusion coefficient, fraction of mobile clusters, and/or confinement radius (Fig. 2D, E, movie S4), while pLAT → N-WASP clusters had a tendency to align with actin filaments and showed a decrease in the fraction of mobile clusters and confinement radius (Fig. 2D, E, movie S4). pLAT → Nck clusters exhibited an intermediate behavior, with a slight increase in the fraction of mobile clusters and their apparent diffusion

coefficient, but at the same time a decrease in the confinement radius of confined and immobile clusters (Fig. 2D, E, movie S4). pLAT → Nck clusters also tended to align with actin filaments, although to a lesser degree than clusters containing N-WASP (Figure 2B, C). When clusters were formed within active actomyosin networks, all cluster compositions exhibited an overall increase in mobility (larger mobile fraction, apparent diffusion coefficient, and/or confinement radius). The increase for pLAT → Sos1 and pLAT → pSLP76 clusters was subtle, larger for pLAT → Nck clusters, and largest for pLAT → N-WASP clusters. The influence of actomyosin on pLAT→ N-WASP clusters was generally in the opposite direction of the influence of actin alone (Fig. 2D, E, movie S5). These data suggest that clusters containing Nck and Nck/N-WASP, which wet filaments and show a large differential in behavior between actin alone and actomyosin conditions, can be viewed distinctly from clusters containing Sos1 or Sos1/pSLP76, which do not wet filaments and show small differences between the two types of actin network.

To further investigate the ability of clusters to move with actin filaments, we performed experiments where a membrane-associated actin network was induced to contract into asters by addition of myosin II filaments in the presence of low concentrations of salt and ATP (see Supplemental Methods). These actomyosin contraction experiments were performed with pLAT → Sos1 and pLAT → N-WASP clusters. Initially, pLAT → Sos1 clusters were randomly distributed on the membrane while pLAT → N-WASP clusters were aligned along the actin filaments as observed above (Fig. 3A). In both cases the filament network started to contract instantly upon myosin II addition, and formed stable asters within 2 minutes (movie S6). As shown in Figure 3A, at the end of the contraction most of the pLAT → Sos1 clusters remained scattered across the bilayer, while virtually all of the pLAT → N-WASP clusters had moved with the actin into asters. To quantify these behaviors, we examined the speed and direction of both cluster movement and actin movement during actomyosin network contraction using Spatio-Temporal Image Correlation Spectroscopy (STICS) (*29*) (Fig. 3B). We found that the speed of

pLAT → Sos1 clusters was largely independent of the speed of actin, while the speed of pLAT → N-WASP clusters correlated well with the speed of actin (Fig. 3C). Additionally, the distribution of angles between the vectors of pLAT → N-WASP cluster movement and proximal actin movement showed clear preference for smaller angles, indicating a high degree of co-movement. In contrast, the angle distribution for pLAT → Sos1 clusters showed only a slight preference for smaller angles that was marginally significant (Fig. 3D). Together, the steady state (Fig. 2) and contraction (Fig. 3) experiments and analyses show that LAT clusters are influenced by actin network dynamics in a composition-dependent fashion. Clusters containing Nck or N-WASP bind to and move with actomyosin filaments. In contrast, clusters lacking these proteins do not bind filaments appreciably, and are likely moved by non-specific steric contacts. Thus, Nck and N-WASP function as molecular clutches between LAT clusters and actin.

Basic regions of Nck and N-WASP couple LAT clusters to actin filaments

The data above suggest that Nck and N-WASP mediate binding of clusters to actin filaments. To test this, we quantified the recruitment of preformed actin filaments to lipid bilayers by pLAT clusters of different compositions in the absence of eABD. As shown in Figure 4A, only clusters containing Nck or Nck and N-WASP recruited substantial amounts of actin filaments. In both cases, clusters were deformed and elongated along filaments, as observed above.

We next performed co-sedimentation assays to determine whether Nck or N-WASP could bind actin filaments in solution or whether efficient binding required the proteins to be arrayed on a two-dimensional surface. Nck did not appreciably co-sediment with actin filaments. Consistent with previous reports, N-WASP did bind filaments (*24*), although not to the same degree as α-actinin, a high-affinity actin filament-binding protein (Fig. S3). To identify the elements of Nck that mediate pLAT cluster binding to actin filaments, we attached polyhistidine-tagged fragments of Nck to planar lipid bilayers and measured their ability to recruit actin filaments from solution.

Nck is composed of three SH3 domains and an SH2 domain, connected by flexible linkers of 25-42 residues (*30*). Of these seven elements, two contain dense basic patches, one contains dense acidic patches, and the remainder are relatively free of dense charge patches. As detailed in Figure S4, Nck fragments containing an excess of basic elements recruited actin to the membrane, where greater excess resulted in more efficient recruitment, while neutral or acidic fragments did not. Similarly, mutating one of the basic elements (the linker between the first and second SH3 domains, L1) to neutralize it ($Nck_{Neutral}$) or to make it acidic (Nck_{Acidic}) greatly impaired actin recruitment, while making it more basic (Nck_{Basic}) enhanced actin recruitment (Fig. 4B, S5). These data indicate that basic regions of Nck likely contribute to binding of phase-separated LAT clusters to actin filaments.

Like Nck, N-WASP also has a central basic region (residues 186-200). We thus asked whether this region and/or the two C-terminal WH2 motifs contribute to coupling of clusters to actin filaments (*24*). We generated pLAT → N-WASP clusters with N-WASP fragments consisting of the basic-proline elements (BP), basic-proline + VCA (BPVCA) elements, and basic-proline + VCA_{mut} ($BPVCA_{mut}$), which contains mutations to the WH2 motifs in the VCA region that impair filament binding (*24*). All three cluster types strongly recruited actin, indicating that WH2-actin interactions are not needed for actin recruitment in the context of LAT clusters (Fig. S6). To further examine the basic region, we generated three variants of His_6-tagged full length N-WASP (fused N-terminally to the WASP-binding region of WIP to afford stability; Fig. S7): N-WASP containing a doubled basic region ($N\text{-}WASP_{Basic}$), wild-type N-WASP ($N\text{-}WASP_{WT}$) and N-WASP containing a neutral linker instead of the basic region ($N\text{-}WASP_{Neutral}$). As shown in figures 4C and S7, these variants recruited actin in the order $N\text{-}WASP_{Basic}$ >> $N\text{-}WASP_{WT}$ > $N\text{-}WASP_{Neutral}$. Thus, for both Nck and N-WASP, the degree of positive charge in basic elements strongly correlates with the ability of the proteins and their LAT clusters to recruit actin filaments to membranes.

To test whether these basic region-mediated interactions are necessary to couple cluster movement to actin movement (Fig. 3), we performed actin contraction assays with clusters composed of N-WASP$_{Basic}$ or N-WASP$_{Neutral}$. Before myosin II addition, pLAT -> N-WASP$_{Basic}$ clusters colocalized almost perfectly with actin filaments, while pLAT -> N-WASP$_{Neutral}$ clusters only partially colocalized with actin filaments, consistent with the notion that the basic region mediates binding of clusters to actin filaments (Fig. 4C, D). Similarly, after actin network contraction, pLAT → N-WASP$_{Basic}$ clusters co-localized with actin asters to a similar degree as pLAT → N-WASP$_{WT}$ clusters, while pLAT → N-WASP$_{Neutral}$ clusters did not (Fig. 4D vs. Fig. 3A, movie S7 vs. movie S6). STICS analysis revealed that the correlation of pLAT → N-WASP$_{Basic}$ cluster movement with local actin movement was similar to that of pLAT → N-WASP$_{WT}$ cluster movement, while the correlation of pLAT → N-WASP$_{Neutral}$ cluster movement was worse (Fig. 4E, F). The remaining correlation for pLAT → N-WASP$_{Neutral}$ clusters is most likely due to the presence of Nck in these clusters, which also contributes to clusters binding to actin. Together these data demonstrate that regions of Nck and N-WASP that contain dense basic patches can mediate the clutch-like behaviors of the proteins by directly interacting with actin filaments proportionally to the degree of positive charge, and that these interactions are necessary for clusters to faithfully move with actin.

These data, plus our cellular observation that Nck (and presumably its ligand, WASP, the dominant N-WASP homolog in T cells) dissociates from LAT clusters near the change in actin architecture, suggest a mechanism by which LAT clusters can be moved radially through the action of two actin networks at the IS. In the outer region of the IS, where the clusters contain Nck and WASP, strong adhesion between the clusters and actin filaments enables the clusters to move radially with actin retrograde flow. Release of Nck and WASP from the clusters near the switch to actomyosin arcs changes their interaction with filaments to a potentially non-

specific, steric mode. This enables clusters to be swept toward the center of the synapse by the radial component of movement of the contractile actin arcs, with which they are expected to undergo repeated short, non-specific interactions, without being moved circularly by the telescoping action of the arcs (as would be the case for strong binding to actin filaments).

Constitutive engagement between LAT clusters and actin leads to aberrant cluster movement across the IS

To test this model we sought to alter the adhesion of pLAT clusters to the actin filament network by fusing Grb2, which remains in LAT clusters throughout their trajectories (Fig. 1A-C), with the doubled basic region of N-WASP ($Grb2_{Basic}$). We reasoned that this would generate LAT clusters that bind actin filaments in the absence of Nck or WASP (i.e. clusters that have a constitutive clutch), perturbing their radial movement in the medial region of the IS where they encounter actin arcs. In biochemical assays, membrane-bound pLAT-$Grb2_{basic}$ complex recruited actin filaments, while pLAT alone or the pLAT-$Grb2_{WT}$ complex did not (Fig. 5A). In actomyosin contraction assays, clusters of pLAT/$Grb2_{Basic}$/Sos1 initially wet filaments and then localized to actin asters after myosin II-induced contraction to a greater degree than pLAT/$Grb2_{WT}$/Sos1 clusters, but to a lesser degree than pLAT → N-WASP clusters (Fig. 5B, movie S8 vs. movie S6). Similarly, during actomyosin network contraction the movement of pLAT/$Grb2_{Basic}$/Sos1 clusters was correlated more strongly with actin movement than clusters containing $Grb2_{WT}$ (Fig. S8), but less strongly than pLAT → N-WASP clusters (Fig. 3C, D). Together, these data demonstrate that the double basic motif of N-WASP, when added to Grb2, can act as a molecular clutch coupling clusters to actin.

We next asked whether expression of $Grb2_{Basic}$ in Jurkat T cells would cause changes in the trajectory of LAT clusters at the IS. Cells expressing $Grb2_{Basic}$-mCherry were activated on bilayers as above. Similar to cells expressing $Grb2_{WT}$-mCherry, LAT clusters formed at the

periphery of the IS and retained $Grb2_{Basic}$-mCherry throughout their trajectories to the cSMAC (Fig. 5C). However, in these cells clusters deviated from a straight trajectory to the center of the synapse significantly more frequently than in cells expressing $Grb2_{WT}$-mCherry (Fig. 5D, E, movie S9 vs. S1). This behavior is consistent with abnormally high adhesion of clusters containing $Grb2_{Basic}$ to actin filaments, even after Nck has presumably dissipated, leading to trajectories that reflected the telescoping, circular component of motion of the contractile actin arcs.

Formin activity is necessary for LAT cluster composition change

Finally, we asked whether the transition from the dendritic actin architecture to the contractile arc architecture might play a role in changing the composition of LAT clusters near this location in the IS. Previous data showed that the contractile arcs are generated by the formin mDia1 and could be eliminated by cell treatment with the formin inhibitor, SMIFH2 (*18*). We found that in contrast to control cells treated with DMSO, where Nck dissipated normally from LAT clusters (Fig. 6A and B, Fig. S9, movie S11), cells treated with SMIFH2 for five minutes prior to imaging displayed LAT clusters with virtually constant Nck intensities throughout their trajectories from the periphery to the cSMAC (Fig. 6A and C, Fig. S9, movie S12). Thus, the activity of formin proteins, and perhaps the actin arcs that they generate, act to alter the composition of LAT clusters, likely altering their downstream signaling activities in the central region of the IS. We note that the SMIFH2 data further support the notion that in unperturbed cells, space, rather than time, is the key determinant of Nck residence in clusters (assuming that formin does not also create a temporal signal). Our combined data suggest that the two actin networks in activated Jurkat T cells not only spatially organize the immunological synapse by moving LAT clusters, but may also contribute to creation of specific signaling zones.

Discussion

Our combined in vitro and cellular data suggest a model for movement of LAT clusters across the IS by the cortical actin networks. Clusters form in the outer region of the IS with the full complement of signaling molecules, including Grb2, SOS1, SLP-76, Nck, and WASP. Basic regions on Nck and WASP act as a molecular clutch, enabling the clusters to adhere tightly to the outer dendritic actin network, and travel radially with the network as it moves by retrograde flow. Near the junction with the formin-generated actin arcs, a formin-dependent signal causes loss of Nck, and likely WASP (which is present in clusters through its interactions with Nck). The retention of Nck by the IS clusters in formin-inhibited cells is consistent with this possibility. We do not yet know the nature of this signal, but one straightforward possibility would be dephosphorylation of SLP-76, as Nck is known to join clusters primarily through binding SLP-76 phosphotyrosines (*31*, *32*). More complex mechanisms involving appearance of competing Nck binding partners or mechanical disruptions are also possible. Loss of Nck/WASP dramatically decreases adhesion of the LAT clusters to actin. In this state, it appears that clusters can still be moved by actin, but likely through repeated non-specific steric interactions. This is consistent with previous observations that in the actin arcs region of the IS, clusters are repeatedly hit by arcs that move them briefly but then release (*18*). The circular movement of the telescoping actin arcs is randomly directed clockwise and counterclockwise, and produces no net directional forces on the clusters. But the radial component is consistent, and completes the radial trajectory of the clusters to the center of the IS. When Grb2 is artificially equipped with a basic region, clusters in the central region have a propensity for aberrant movement, likely due to inappropriately strong adhesion to the telescoping actin arcs.

LAT clusters represent one instance of a general class of cellular compartments termed biomolecular condensates, which concentrate macromolecules at discrete sites without a surrounding membrane. It is generally thought that the functions of condensates are intimately connected to their compositions, and that changes in composition could cause changes in

function (*33*). Our data here demonstrate that when Nck and N-WASP are arrayed on membranes they can bind actin filaments efficiently, even though both bind filament sides only weakly in solution. This adhesion enables clusters containing the proteins to be moved over long distances in response to actomyosin contraction. Adhesion is lost when Nck and N-WASP depart. Thus, the composition of LAT clusters plays an important role in their coupling to actin and their mode of movement at the IS. These behaviors of the LAT system are produced by generalizable features of membrane-associated condensates - their high density and composition based on regulatable interactions. Thus, analogous behaviors are likely to be widely observed as the biochemical and cellular activities of other condensates are explored.

References

1. M. Rao, S. Mayor, Active organization of membrane constituents in living cells. *Curr. Opin. Cell Biol.* **29**, 126–132 (2014).
2. E. Sezgin, I. Levental, S. Mayor, C. Eggeling, The mystery of membrane organization: composition, regulation and roles of lipid rafts. *Nat. Rev. Mol. Cell Biol.* **18**, 361–374 (2017).
3. M. F. Garcia-Parajo, A. Cambi, J. A. Torreno-Pina, N. Thompson, K. Jacobson, Nanoclustering as a dominant feature of plasma membrane organization. *J. Cell Sci.* **127**, 4995–5005 (2014).
4. J. M. Githaka *et al.*, Ligand-induced growth and compaction of CD36 nanoclusters enriched in Fyn induces Fyn signaling. *J. Cell Sci.* **129**, 4175–4189 (2016).
5. P. Li *et al.*, Phase transitions in the assembly of multivalent signalling proteins. *Nature*. **483**, 336–340 (2012).
6. S. Banjade, M. K. Rosen, Phase transitions of multivalent proteins can promote clustering of membrane receptors. *Elife*. **3**, e04123 (2014).
7. X. Su *et al.*, Phase separation of signaling molecules promotes T cell receptor signal transduction. *Science (80-.).* **352**, 595–599 (2016).
8. S. F. Banani, H. O. Lee, A. A. Hyman, M. K. Rosen, Biomolecular condensates: organizers of cellular biochemistry. *Nat Rev Mol Cell Biol*. **18**, 285–298 (2017).
9. A. Babich *et al.*, F-actin polymerization and retrograde flow drive sustained PLCγ1 signaling during T cell activation. *J. Cell Biol.* **197**, 775–787 (2012).
10. Y. Yu, N. C. Fay, A. A. Smoligovets, H.-J. Wu, J. T. Groves, Myosin IIA Modulates T Cell Receptor Transport and CasL Phosphorylation during Early Immunological Synapse Formation. *PLoS One*. **7**, e30704 (2012).
11. T. Ilani, G. Vasiliver-Shamis, S. Vardhana, A. Bretscher, M. L. Dustin, T cell antigen receptor signaling and immunological synapse stability require myosin IIA. *Nat Immunol*. **10**, 531–539 (2009).
12. S. Kumari *et al.*, T Lymphocyte Myosin IIA is Required for Maturation of the Immunological Synapse. *Front. Immunol.* **3** (2012), p. 230.
13. K. D. Mossman, G. Campi, J. T. Groves, M. L. Dustin, Altered TCR Signaling from

Geometrically Repatterned Immunological Synapses. *Science (80-.).* **310**, 1191–1193 (2005).

14. Y. Kaizuka, A. D. Douglass, R. Varma, M. L. Dustin, R. D. Vale, Mechanisms for segregating T cell receptor and adhesion molecules during immunological synapse formation in Jurkat T cells. *Proc Natl Acad Sci U S A*. **104**, 20296–20301 (2007).
15. A. L. DeMond, K. D. Mossman, T. Starr, M. L. Dustin, J. T. Groves, T cell receptor microcluster transport through molecular mazes reveals mechanism of translocation. *Biophys J*. **94**, 3286–3292 (2008).
16. C. H. Yu, H. J. Wu, Y. Kaizuka, R. D. Vale, J. T. Groves, Altered actin centripetal retrograde flow in physically restricted immunological synapses. *PLoS One*. **5**, e11878 (2010).
17. J. Yi, X. S. Wu, T. Crites, J. A. Hammer 3rd, Actin retrograde flow and actomyosin II arc contraction drive receptor cluster dynamics at the immunological synapse in Jurkat T cells. *Mol Biol Cell*. **23**, 834–852 (2012).
18. S. Murugesan *et al.*, Formin-generated actomyosin arcs propel T cell receptor microcluster movement at the immune synapse. *J. Cell Biol.* **215**, 383–399 (2016).
19. J. A. Hammer 3rd, J. K. Burkhardt, Controversy and consensus regarding myosin II function at the immunological synapse. *Curr Opin Immunol*. **25**, 300–306 (2013).
20. A. Ponti, M. Machacek, S. L. Gupton, C. M. Waterman-Storer, G. Danuser, Two distinct actin networks drive the protrusion of migrating cells. *Science (80-.).* **305**, 1782–1786 (2004).
21. A. Ponti *et al.*, Periodic patterns of actin turnover in lamellipodia and lamellae of migrating epithelial cells analyzed by quantitative Fluorescent Speckle Microscopy. *Biophys J*. **89**, 3456–3469 (2005).
22. K. Jaqaman *et al.*, Robust single-particle tracking in live-cell time-lapse sequences. *Nat. Methods*. **5**, 695 (2008).
23. M. Barda-Saad *et al.*, Dynamic molecular interactions linking the T cell antigen receptor to the actin cytoskeleton. *Nat Immunol*. **6**, 80–89 (2005).
24. C. Co, D. T. Wong, S. Gierke, V. Chang, J. Taunton, Mechanism of actin network attachment to moving membranes: barbed end capture by N-WASP WH2 domains. *Cell*. **128**, 901–913 (2007).
25. P. Bieling *et al.*, WH2 and proline□rich domains of WASP□family proteins collaborate to accelerate actin filament elongation. *EMBO J.* **37**, 102–121 (2018).
26. D. V. Köster *et al.*, Actomyosin dynamics drive local membrane component organization in an in vitro active composite layer. *Proc. Natl. Acad. Sci.* **113**, E1645–E1654 (2016).
27. K. Jaqaman *et al.*, Cytoskeletal control of CD36 diffusion promotes its receptor and signaling function. *Cell*. **146**, 593–606 (2011).
28. A. R. Vega, S. A. Freeman, S. Grinstein, K. Jaqaman, Multistep Track Segmentation and Motion Classification for Transient Mobility Analysis. *Biophys. J.* **114**, 1018–1025 (2018).
29. G. W. Ashdown, A. Cope, P. W. Wiseman, D. M. Owen, Molecular flow quantified beyond the diffraction limit by spatiotemporal image correlation of structured illumination microscopy data. *Biophys J*. **107**, L21-3 (2014).
30. S. Banjade *et al.*, Conserved interdomain linker promotes phase separation of the multivalent adaptor protein Nck. *Proc. Natl. Acad. Sci.* **112**, E6426–E6435 (2015).
31. M. Barda-Saad *et al.*, Cooperative interactions at the SLP-76 complex are critical for actin polymerization. *Embo J*. **29**, 2315–2328 (2010).
32. M. H. Pauker, N. Hassan, E. Noy, B. Reicher, M. Barda-Saad, Studying the Dynamics of SLP-76, Nck, and Vav1 Multimolecular Complex Formation in Live Human Cells with Triple-Color FRET. *Sci Signal*. **5**, 1–9 (2012).
33. S. F. Banani *et al.*, Compositional Control of Phase-Separated Cellular Bodies. *Cell*. **166**, 651–663 (2016).

Figure Legends

Figure 1. LAT cluster composition changes as clusters move across the IS.

(A) TIRF microscopy image of Jurkat T cell expressing Grb2-mCherry (magenta in merge) and LAT-mCitrine (green in merge) activated on a planar lipid bilayer coated with OKT3 and ICAM-1. Scale Bar = 5 μm. **(B)** Magnification of boxed region in (A), with normalized radial position (1 at synapse edge, 0 at cSMAC center) indicated above images. Scale bar = 2 μm. **(C)** Quantification of fluorescence intensity ratios of Grb2 / LAT (orange) and Nck / LAT (blue) in clusters in Jurkat T cells at different normalized radial positions. Measurements were made at identical relative locations but data points are slightly offset in the graph for visual clarity. Plot displays median and notches from boxplot for 95% confidence interval from 207 clusters from 36 cells from N = 5 independent experiments. Only tracks in which the Grb2 or Nck intensity was greater than 1 standard deviation above background during the first three measurements were used to generate this plot. **(D)** TIRF microscopy image of Jurkat T cell expressing Nck-sfGFP (green in merge) and LAT-mCherry (magenta in merge) activated on a planar lipid bilayer by OKT3 and ICAM-1. Scale Bar = 5 μm. **(E)** Magnification of boxed region in (D). Scale bars and details as in (B).

Figure 2. Cluster composition regulates cluster movement with actin networks.

(A) Schematic of biochemical reconstitution in solutions containing LAT and eABD attached to planar lipid bilayers and LAT clustering agents, actin filaments, and myosin filaments in solution. **(B)** TIRF microscopy images of pLAT clusters of the indicated compositions (see text for nomenclature) without actin (left column), with actin-only networks (middle column), or with actomyosin networks (right column). pLAT-Alexa488 is green, rhodamine-actin filaments are magenta. Scale bar = 5 μm. **(C)** Actin enrichment at clusters, the ratio of actin fluorescence intensity within clusters to actin intensity outside clusters (see Methods). Error bars indicate

mean +/- s.d. from N = 5 replicates from each of 3 independent experiments (15 FOV total). **(D)** Example plots of cluster tracks colored based on their movement type, as classified by Moment Scaling Spectrum analysis. Black = immobile, green = confined, and cyan = mobile. Scale bar = 5 μm. **(E)** (top) Fraction of the indicated cluster mobility types in the absence of actin (blue), in the presence an actin-only network (red), or in the presence of an active actomyosin network (gold). (middle) Effective diffusion coefficients of the clusters categorized and colored as in top row. (bottom) Confinement radius of the clusters categorized and colored as in top row. P-values are for indicated distribution comparisons via Wilcoxon rank-sum test with Bonferroni correction.

Figure 3. pLAT → N-WASP clusters bind to and move with moving actin filaments.

(A) TIRF microscopy images of pLAT → Sos1 clusters (left two columns) and pLAT → N-WASP clusters (right two columns) formed in an actin network before (t = 0 min) and two minutes after (t = 2 min) addition of myosin II. pLAT clusters are green and actin is magenta in merge. Scale bar = 5 μm. **(B-D)** STICS analysis of actin and cluster movement. **(B)** Representative map of actin and cluster vector fields. Green arrows indicate cluster movement, magenta arrows indicate actin movement. Lower panels show expansions of upper panels. **(C)** Cluster speed vs. actin speed at same position. Cluster type indicated above each heat map. Heat map indicates frequency in each bin, i.e. counts in each bin normalized by total number of counts. Data pooled from 5 fields of view in each of 3 independent experiments (15 FOV total). **(D)** Distribution of the angle between actin and cluster movement vectors for pLAT → Sos1 (blue), pLAT → N-WASP (gold), randomized pLAT → Sos1 (red) and randomized pLAT → N-WASP (purple) (see Methods for randomization). N = 5 replicates from each of 3 independent experiments (15 FOV total). P-values are for indicated distribution comparisons via Kolmogorov-Smirnov test.

Figure 4. Basic regions of Nck and N-WASP mediate interaction of clusters and actin filaments.

(A) (Left) TIRF microscopy images of rhodamine-actin (magenta) recruited to planar lipid bilayers by the indicated pLAT cluster types (green). Scale bar = 5 μm. (Right) Normalized total rhodamine-actin fluorescence intensity on planar lipid bilayers. Error bars indicate mean +/- s.d. from N = 5 replicates from each of 3 independent experiments (15 FOV total). **(B)** (left) TIRF microscopy images of rhodamine-actin recruited to planar lipid bilayers by His-tagged Nck variants. (right) Normalized average actin intensity on planar lipid bilayers. Error bars indicate mean +/- s.d. from N = 5 replicates from each of 3 independent experiments (15 FOV total). **(C)** (left) TIRF microscopy images of rhodamine-actin recruited to planar lipid bilayers by His-tagged N-WASP variants. Error bars indicate mean +/- s.d. N = 5 replicates from each of 3 independent experiments (15 FOV total). **(D)** (Left) TIRF microscopy images of pLAT → $N\text{-}WASP_{Basic}$ clusters (left two columns) and LAT → $N\text{-}WASP_{Neutral}$ clusters (right two columns) formed in an actin network before (t = 0 min) and two minutes after (t = 2 min) addition of myosin II. pLAT clusters are green and actin is magenta in merge. Scale bar = 5 μm. **(E)** Cluster speed vs. actin speed at same position from STICS analysis. Cluster type indicated above each heat map. Heat map indicates frequency in each bin (as in Fig. 3C). N = 5 replicates from each of 3 independent experiments (15 FOV total). **(F)** Distribution of the angle between actin and cluster movement vectors for pLAT → $N\text{-}WASP_{Basic}$ (gold), randomized LAT → $N\text{-}WASP_{Basic}$ (purple), pLAT → $N\text{-}WASP_{WT}$ (black, same data as in Fig. 3), pLAT → $N\text{-}WASP_{Neutral}$ (blue), and randomized LAT → $N\text{-}WASP_{Neutral}$ (red). N = 5 replicates from each of 3 independent experiments (15 FOV total). P-values are for indicated distribution comparisons via Kolmogorov-Smirnov test.

Figure 5. Grb2 fused to a basic molecular clutch can couple clusters to actin

(A) TIRF microscopy images of rhodamine-actin recruited to planar lipid bilayers by His-tagged pLAT or clusters of pLAT → Grb2 or pLAT → $Grb2_{Basic}$. Scale bar = 5 μm. **(B)** TIRF microscopy images of pLAT → Sos1 clusters containing $Grb2_{WT}$ (top row; data from Fig. 3) or $Grb2_{Basic}$ (bottom row) formed in an actin network before (t = 0 min) and two minutes after (t = 2 min) addition of myosin II. Actin shown in magenta and pLAT clusters in green. Scale bar = 5 μm. **(C)** TIRF microscopy image of Jurkat T cell expressing Grb2-mCherry (top, magenta in merge) or $Grb2_{Basic}$-mCherry (bottom, magenta in merge) and LAT-mCitrine (green in merge) activated on a planar lipid bilayer coated with OKT3 and ICAM-1. Scale Bar = 5 μm. **(D)** Trajectories of LAT clusters in Jurkat T cells expressing Grb2-mCherry (top) or $Grb2_{Basic}$-mCherry (bottom) recorded over 2 to 5 minutes of imaging. Trajectories are color-coded as indicated in the legend at right according to deviation from a straight line between the estimated starting point of actin engagement and just before entering the cSMAC (see Methods). Scale bar = 5 μm. **(E)** Distribution of deviations from a straight line for clusters in Jurkat T cells expressing Grb2-mCherry (red) or $Grb2_{Basic}$-mCherry (blue). N = 207 clusters from 23 cells from 7 individual experiments. P-value is for comparing the two distributions via a Kolmogorov-Smirnov test. **(F)** Fluorescence intensity ratios of Grb2 / LAT in clusters (blue, data from Figure 1C) or $Grb2_{Basic}$ / LAT clusters (orange) at different normalized radial positions. Measurements were made at identical relative locations but data are slightly offset in the graph for visual clarity. Plot displays median and notches from boxplot for 95% confidence interval from N = 207 clusters from 23 cells from 7 individual experiments. Only tracks in which the Grb2 or $Grb2_{Basic}$ intensity was greater than 1 standard deviation above background during the first three measurements were used to generate this plot.

Figure 6. Formin activity is necessary for Nck dissipation from LAT clusters.

(A) Fluorescence intensity ratios of Nck / LAT in clusters in Jurkat T cells treated with DMSO (blue) or the formin inhibitor, SMIFH2, (orange) at different normalized radial positions.

Measurements were made at identical relative locations but data are slightly offset in the graph for visual clarity. Plot displays median and notches from boxplot for 95% confidence interval from N = 145 clusters from 25 cells from 5 individual experiments. Only tracks in which the Nck intensity was greater than 1 standard deviation above background during the first three measurements were used to generate this plot. The first DMSO data point (Normalized Radial Position = 1) does not appear in the plot because there were not enough clusters detected to generate a statistically significant point. **(B, C)** Magnification of boxed regions from Fig. S10 of clusters containing LAT-mCherry (magenta in merge) and Nck-sfGFP (green in merge) during their trajectories across the IS in a cell treated with DMSO **(B)** or SMIFH2 **(C)**. Normalized radial position indicated above image panels. Scale bar = 2 μm.

Figure 1. LAT cluster composition changes as clusters move across the IS.

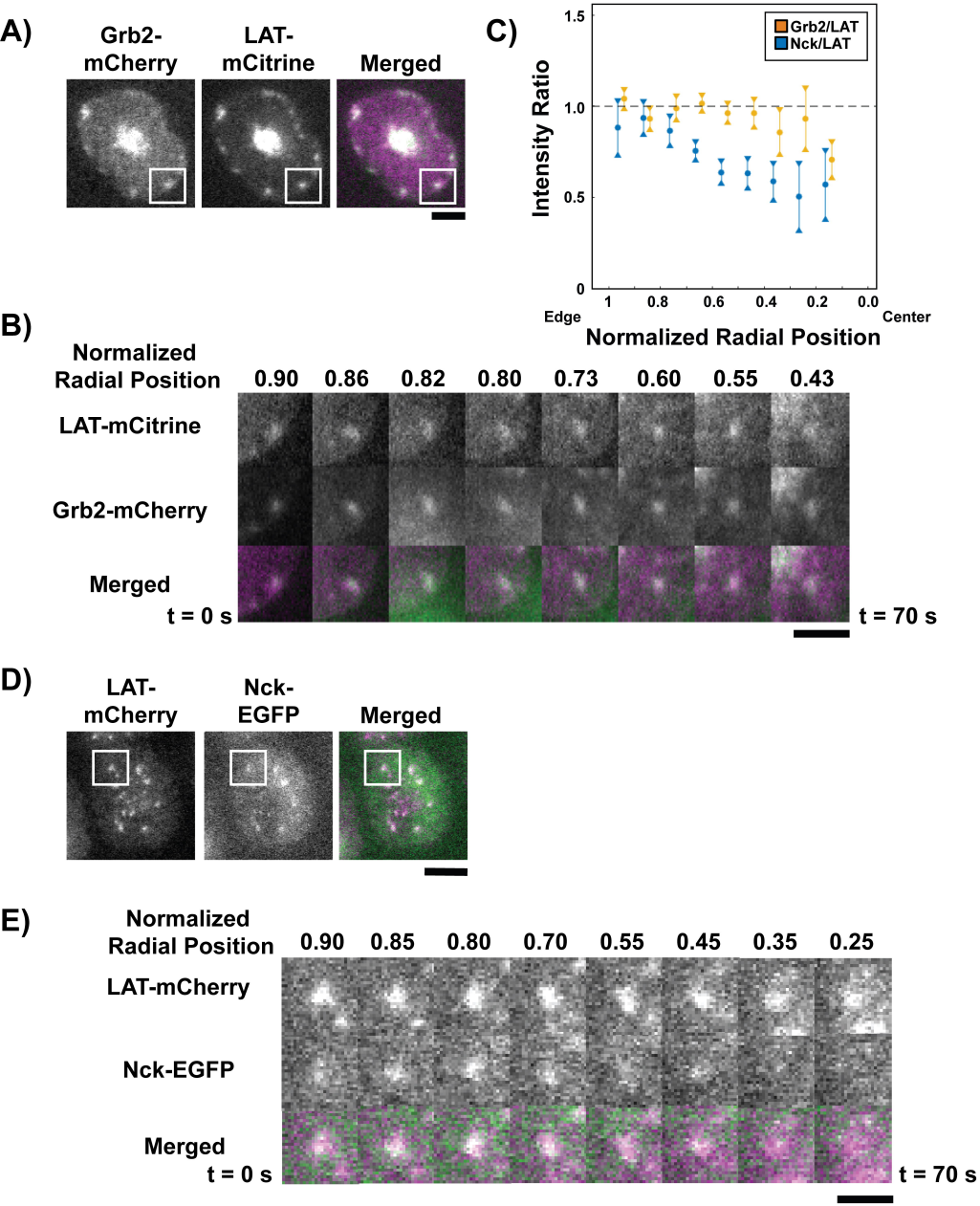

Figure 2. Cluster composition regulates cluster movement with actin networks.

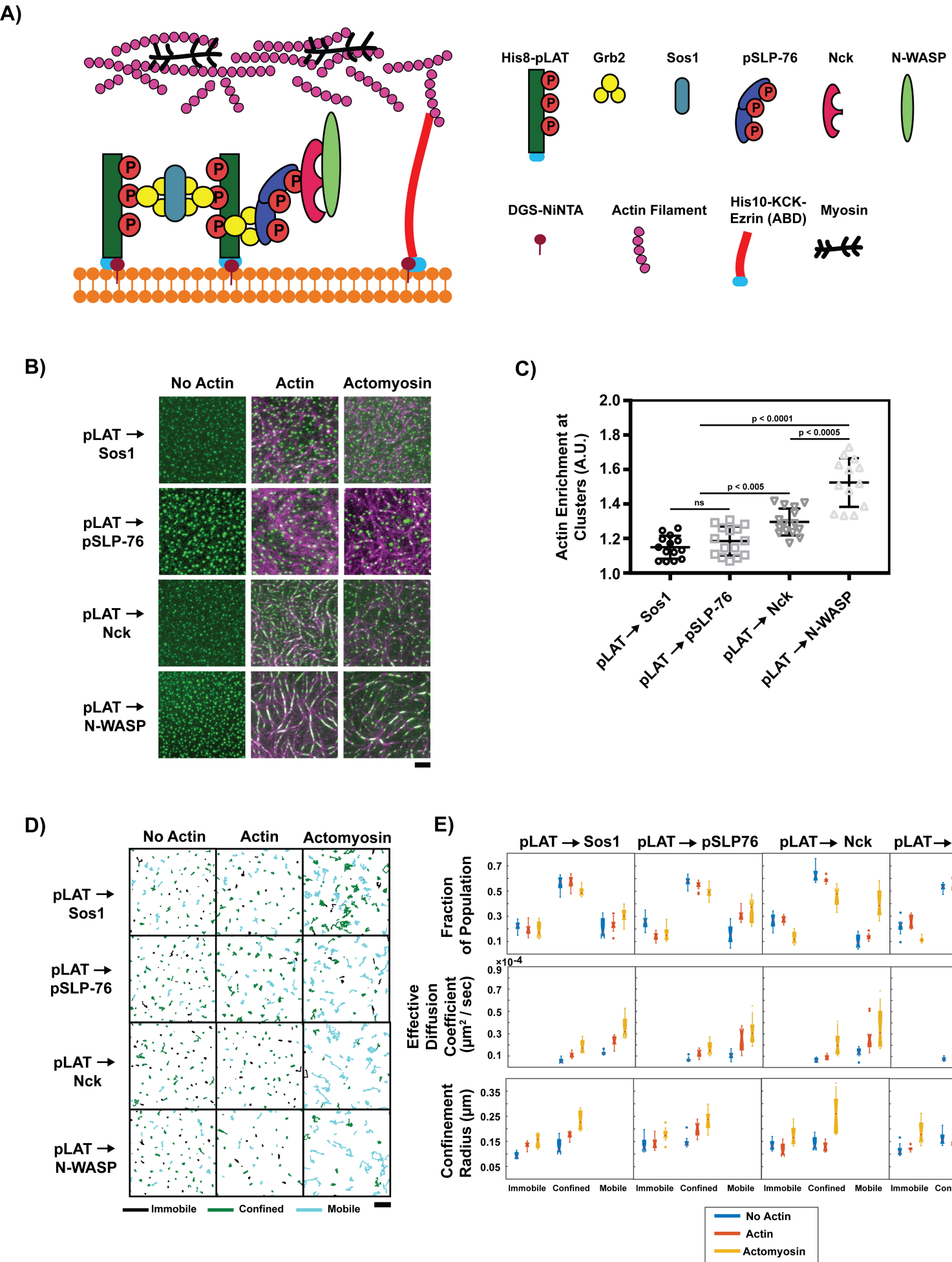

Figure 3. pLAT → N-WASP clusters bind to and move with moving actin filaments.

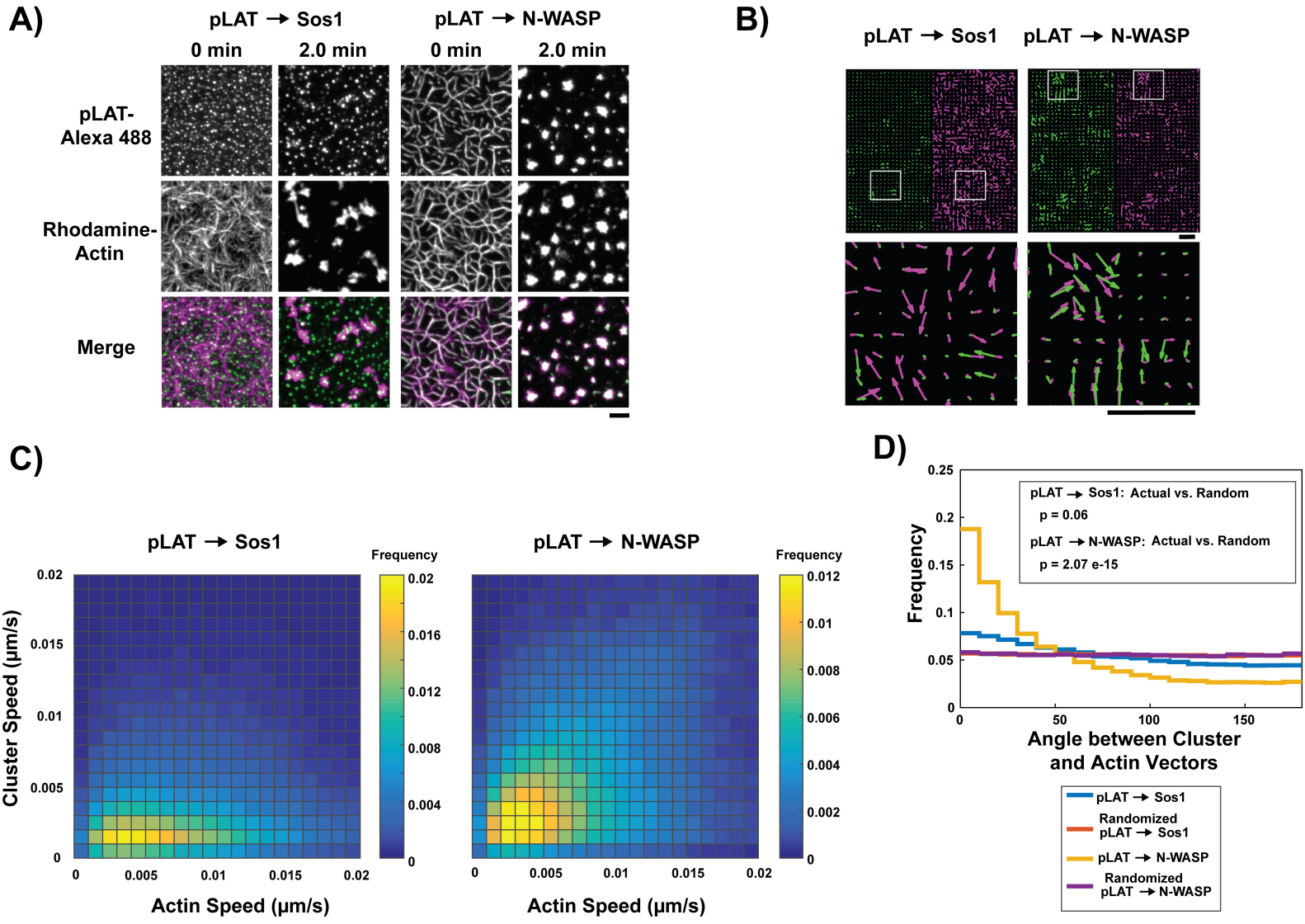

Figure 4. Basic regions of Nck and N-WASP mediate interaction of clusters and actin filaments.

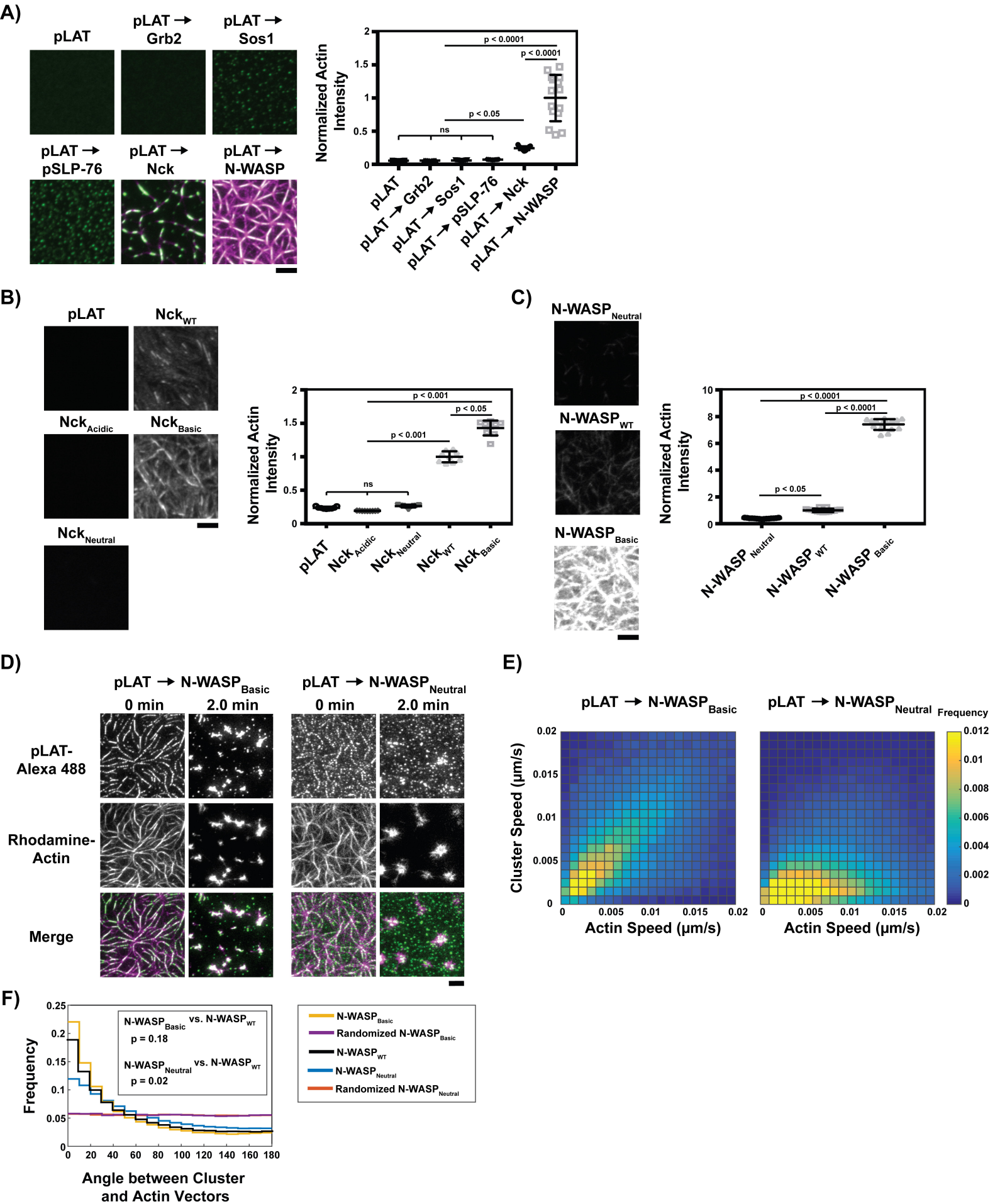

Figure 5. Grb2 fused to a basic molecular clutch can couple clusters to actin

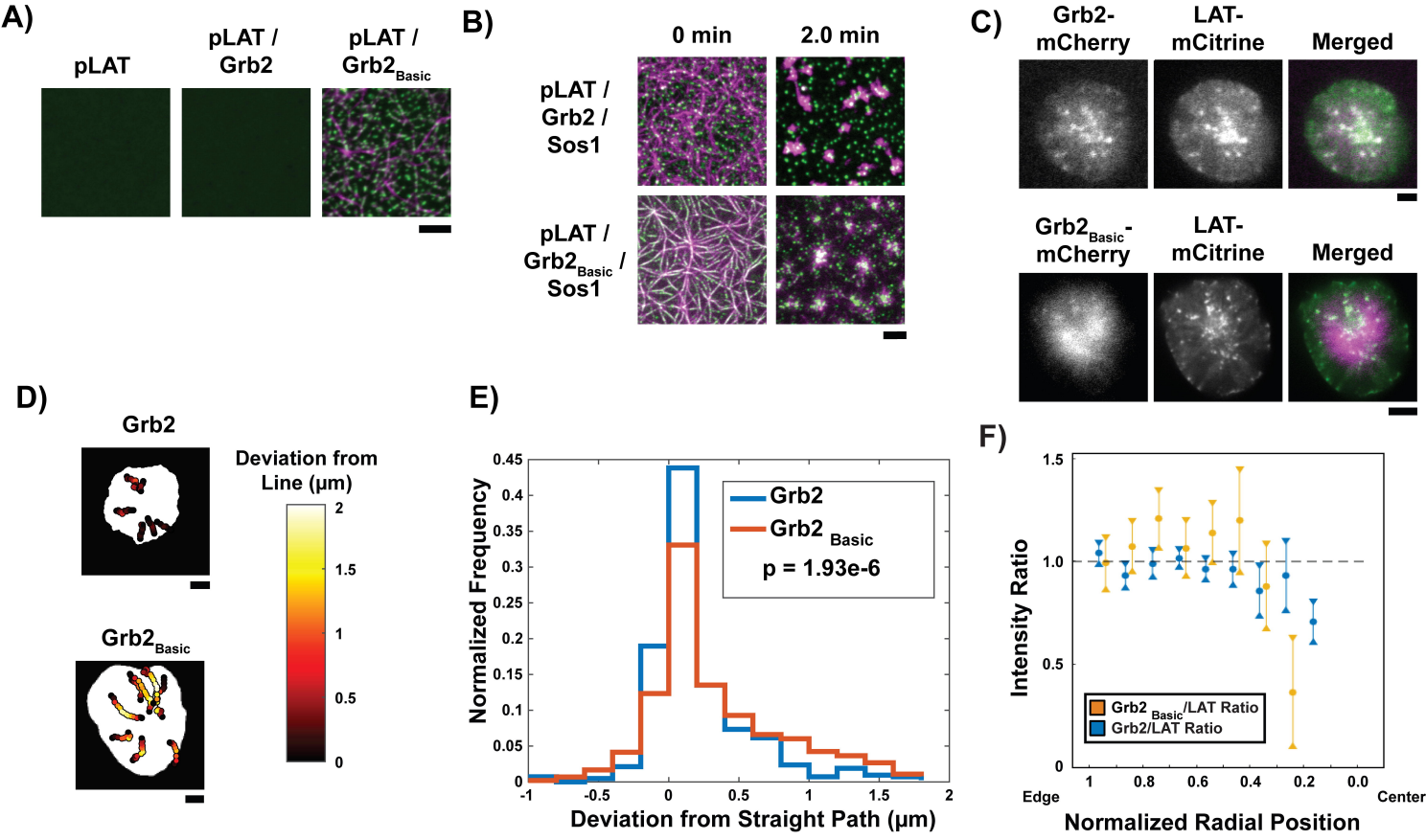

Figure 6. Formin activity is necessary for Nck dissipation from LAT clusters.